VARIATIONS IN THE INTERPLANETARY

MAGNETIC FIELD: MARINER 2

Part 3. Some Effects upon Solar Cosmic Rays

Paul J. Coleman, Jr.

Publication Number 514

Institute of Geophysics and Planetary Physics

University of California, Los Angeles

Los Angeles 24, California

May 12, 1966

Preprint

Abstract

32640

The observed properties of the variations in the interplanetary field, described in Part 1, are employed in developing a model for the typical interplanetary field. Some properties of the behavior of solar protons in the model field are determined. It is shown that protons with energies less than 1 Mev would travel adiabatically throughout the solar system, protons with energies in the range 1-100 Mev would first encounter efficient scattering at heliocentric ranges beyond 1 AU, protons with energies in the range 100 Mev - 1 bev would encounter efficient scattering at ranges near 1 AU, and protons with energies greater than 1 bev would first encounter efficient scattering at ranges less than 1 AU. It is argued that various properties of solar-proton events may be accounted for by this model. However, non-relativistic solar-flare electrons would travel adiabatically throughout interplanetary space. From measurements described in Part 1, it is shown that a good deal of the observed spread in the directions of travel of solar protons in the interplanetary field at the onset of an event is probably due to the variations in the orientation of the field rather than to a spread in particle pitch angles.

VARIATIONS IN THE INTERPLANETARY

MAGNETIC FIELD: MARINER 2

Part 3. Some Effects upon Cosmic Rays

Paul J. Coleman, Jr.

Institute of Geophysics and Planetary Physics

University of California, Los Angeles

Los Angeles 24, California

Introduction

In Part 1 [Coleman, 1966], some typical properties of variations in the interplanetary magnetic field were described. In this third part, a simple model for the 'average' interplanetary field will be described. This model consists of a superposition of a constant field, with the spiral configuration of the model of Parker [1958], and a zero-mean, time dependent perturbation field with statistical properties at 1 AU as indicated by the results presented in Part 1.

With the model established, the behavior of energetic solar protons in such a field will be examined. In particular, the heliocentric range at which a proton of a given energy would encounter the greatest scattering will be determined for a wide range of proton energies.

As in Part 1, a point in interplanetary space will be described in terms of spherical, polar coordinates r, θ, and ϕ.

For the heliocentric coordinate system used here, the sun's axis of rotation is the polar axis. The colatitude, θ, is measured from the north pole of the sun. Thus, the vector, $\vec{\Omega}_S$, representing the angular momentum of the sun is coincident with the polar axis. The components of the magnetic field, $\vec{B}$, at the point (r, θ, ϕ) are then B_r, B_θ, and B_ϕ, with B_r radially outward from the sun, B_ϕ parallel to $\vec{\Omega}_S \times \vec{r}$ where $\vec{r}$ is the radius vector from the center of the sun to the point (r, θ, ϕ), and B_θ completing the usual right-handed system.

A Model for the Interplanetary Field

The observations of the interplanetary field described in Part 1 provide information concerning the field in only a relatively limited part of interplanetary space. Since solar cosmic rays are affected initially by the fields between the sun and the point of observation, we will require a model for the field throughout interplanetary space.

Any model for this quiet field must exhibit, at 1 AU, characteristics which are consistent on the average with the spiral-field model and which, over shorter periods, are consistent with the temporal variations described in Part 1. The model for the interplanetary medium that will be employed here includes a perfectly conducting solar wind plasma, expanding freely beyond a heliocentric range $r = r_o$ at radial velocity V_p. The average magnetic field at r_o is directed radially with magnitude B_{so}. This model is just that employed by Parker [1958] in predicting the existence of the spiral-field configuration in interplanetary space.

Superimposed on this average background field, is a perturbation field $\vec{b}_o$. The field at (r_o, θ, ϕ), at time t, is subsequently carried out from the sun as a field frozen into the expanding solar wind, thus providing the magnetic field at (r, θ, ϕ) at time $t + \Delta t$, where $\Delta t = (r-r_o)/V_p$.

As mentioned previously, the average field at (r_o, θ, ϕ)

which is radial, will be denoted by $B_{so} \equiv \hat{e}_r B_{so}$. The perturbation field at (r_o, θ, ϕ), which has been denoted $\vec{b}_o$, is

$$\vec{b}_o = \hat{e}_r b_{or} + \hat{e}_\theta b_{o\theta} + \hat{e}_\phi b_{o\phi} \tag{1}$$

The symbol, $\hat{e}_i$, will be employed subsequently to denote a unit vector in the 'i' direction. The magnitudes of the components will be expressed as Fourier integrals of the form

$$\begin{aligned} b_{oi} &= b_{oi}\,(\theta, \phi, t) \\ &= \int_{f_o}^{f_N} a_i \cos\,[2\pi ft + (2\pi\theta/\Delta_{\theta i}) + (2\pi\phi/\Delta_{\phi i}) + \delta_{fi}]df \end{aligned} \tag{2}$$

for $i = r, \theta, \phi$. Here a_i, Δ_θ, and Δ_ϕ are functions of f, and δ_{fi} is an arbitrary constant for each (f, i). The limits of the integration will be determined presently.

With the field specified at (r_o, θ, ϕ, t), the field in interplanetary space at heliocentric ranges beyond r_o can be determined under the assumption that the fields in the perfectly conducting, freely expanding solar wind are just those carried outward from the sun, as a consequence of the relation $(\partial\vec{B}/\partial t) = \nabla \times (\vec{V} \times \vec{B})$ for a perfectly conducting medium. Thus, consider an element of area at r_o. The plasma ejected radially from the area at velocity V_p in the time dt defines an element of volume which exhibits the strain effects of a shear in the negative ϕ direction, along surfaces of constant r. Thus, a radial field B_{or} at (r, θ, ϕ, t) will produce, at $(r, \theta, \phi, t + \Delta t)$, a field with the direction and relative magnitude required by the spiral-field model, i.e., a field with a radial component $(r_o/r)^2 B_{or}$ and an azimuthal component

$$-(r_o/r)^2 \ (\Omega_S/V_p) \ (r-r_o) \ (\sin \theta) B_{or} = -(\tan \alpha_p) \ (r_o/r)^2 B_{or}$$

Here $\Delta t = (r-r_o)/V_p$. A field of magnitude $B_{o\theta}$ in the θ direction at (r_o, θ, ϕ, t) will produce a field of magnitude $(r_o/r)B_{o\theta}$ in the same direction at $(r, \theta, \phi, t + \Delta t)$. Similarly, a field $B_{o\phi}$ in the ϕ direction at (r_o, θ, ϕ, t) will produce a field of magnitude $(r_o/r)B_{o\phi}$ in the same direction at $(r, \theta, \phi, t + \Delta t)$. Thus, the field $\vec{B}(r, \theta, \phi, t)$ will have components

$$\begin{aligned} B_r &= (r_o/r)^2 B_{or}(\theta, \phi, t-\Delta t) \\ B_\theta &= (r_o/r) \ B_{o\theta}(\theta, \phi, t-\Delta t) \qquad (3) \\ B_\phi &= -(r_o/r)^2 \tan \alpha_p \ B_{or}(\theta, \phi, t-\Delta t) + (r_o/r)B_{o\phi}(\theta, \phi, t-\Delta t) \end{aligned}$$

where $\Delta t = (r-r_o)/V_p$, and where the components of the field $\vec{B}_o(\theta, \phi, t)$ at the point (r_o, θ, ϕ) at time t are

$$
\begin{aligned}
B_{or} &= B_{so} + b_{or} \\
B_{o\theta} &= b_{o\theta} \\
B_{o\phi} &= b_{o\phi}
\end{aligned}
\tag{4}
$$

In our model, B_{so} is a constant and the perturbation field $\vec{b}_o$ has components given by Equations 2. Note that the average value of $\vec{B}_\theta$ is assumed to be zero despite some evidence, described in Part 1, for a small positive value. For convenience, the argument of the cosine function sometimes will be written $2\pi f \eta_i + \delta_{fi}$, where

$$
\eta_i = \eta_i(\theta, \phi, t) = t + (\theta/f\Delta_{\theta i}) + (\phi/f\Delta_{\phi i}) \tag{5}
$$

If the motion of the spacecraft is neglected, the magnetometer measures $\vec{B}(r, \theta, \phi, t)$ at the point (r, θ, ϕ). For our purposes, only the values of the quantities B_{so} and $a_i(f)$ will be required, since knowledge of the specific phase differences between the frequency components is not important here. However, knowledge of the gradients of the field in interplanetary space is necessary. The radial gradients of the irregularities, for a specific value of V_p, may be determined from the values of f. In order to specify the gradients in the other two directions, the values of $\Delta_{\theta i}$ and $\Delta_{\phi i}$ must be specified. At this point, our only recourse is a heuristic choice of these values.

Suppose, for example, we required that the perturbation field produce irregularities which are, on the average, isotropic at any point on the surface (r_o, θ, ϕ). First, the magnitudes of the r, θ, and ϕ components of the perturbation field must be equal, i.e., we required that $a_r(f) = a_\theta(f) = a_\phi(f)$. Next, the gradients of the irregularities must be the same in all three directions. This requirement establishes the dependences of $\Delta_{\theta i}$ and $\Delta_{\phi i}$ upon the frequency f. Now the characteristic length, measured in the radial direction, of the disturbance produced at the frequency f is just $\lambda(f) = V_p/f$. If the characteristic lengths of variations measured at a point (r_o, θ, ϕ) in the θ and ϕ directions are to equal $\lambda(f)$, the function $\Delta_{\theta i}(f)$ is determined by $r_o \Delta_{\theta i}(f) = \lambda(f)$ and the function $\Delta_{\phi i}(f)$ is determined by $r_o(\sin\theta)\Delta_{\phi i}(f) = \lambda(f)$. Thus,

$$\Delta_{\theta i}(f) = V_p/fr_o$$

and

$$\Delta_{\theta i}(f) = V_p/fr_o \sin\theta$$

Under these conditions the field $\vec{b}_o$ satisfies, at all points on the surface (r_o, θ, ϕ), the requirements that the average gradients of all three components of the perturbation field are the same and that, for each component, the average gradients in the three directions are the same. Now this model requires that the temporal variations of $B_r(r, \theta, \phi, t)$ be a factor of (r_o/r) smaller than those of $B_\theta(r, \theta, \phi, t)$. However, the measured field exhibits about the same power levels in the variations of all three components of the field. Thus, the simple model of homogeneous magnetic turbulence produced at the source of the solar wind and carried outward as fields frozen into the solar wind is evidently not realistic.

Consider a simple model in which a relatively stable field configuration is established on the surface at r_o which rotates with the sun at angular velocity Ω_S. Let this distribution include the usual constant radial component of magnitude B_{so} and spatially varying components

$$b_{oi} = b_{oi}(\theta', \phi') = \int a_i \cos [(2\pi\theta'/\Delta_{\phi i}) + (2\pi\phi'/\Delta_{\phi i}) + \delta_{fi}]df \qquad (6)$$

$$i = r, \theta, \phi$$

where, as we will see, a_i and the first two terms of the argument of the cosine are functions of f. If we transform into the fixed, heliocentric, solar equatorial system in which $\theta' = \theta$ and $\phi' = \phi + \Omega_S t$, this expression becomes

$$b_{oi} = b_{oi}(\theta, \phi, t) \qquad (7)$$

$$= \int a_i \cos [2\pi\Omega_S t/\Delta_{\phi i}) + (2\pi\theta/\Delta_{\theta i}) + (2\pi\phi/\Delta_{\phi i}) + \delta_{fi}]df$$

$$i = r, \theta, \phi$$

where, by comparison with Equations 2, $f = \Omega_S/\Delta_{\phi i}$. If we require, for each vector component at $(r_o, \pi/2, \phi)$, that the gradients of irregularities measured in the ϕ direction be the same as those measured in the θ direction, we have $\Delta_{\theta i} = \Delta_{\phi i}$. If we require also that the increments $\Delta_{\theta i}$ and $\Delta_{\phi i}$ be sub-multiples of 2π, so that b_{oi} averaged over θ' or ϕ' is identically zero, we have $\Delta_{\theta i} = \Delta_{\phi i} = 2\pi/n$. Then the Fourier integral may be replaced by a Fourier series in the frequencies $f = n\Omega_S/2\pi$. Here n runs from one to N, where N is the greatest integer less than $f_N/(\Omega_S/2\pi)$ and f_N is the Nyquist frequency corresponding to the sampling rate of the magnetometer. In this case, $f_N/\Omega_S 2\pi = 29,255.8$, so that N = 29,255. It should be emphasized that this boundary condition is employed in order to simplify the calculations that follow. It is not necessarily justifiable on physical grounds. For that matter, the assumption that a field configuration, at $r = r_o$, is actually stable in the frame of reference rotating with the sun, is not to be taken seriously. It is employed here only as a convenient way to describe a source for a field $\vec{b}(r, \theta, \phi, t)$ that is continuous in space and time and has vector components with normal distributions of amplitudes, continuous distributions of frequencies, and independent and random phases of the frequency components. Thus, each vector component, $b_i(t)$, at a point in space is actually regarded as the output of a Gaussian random process. The specialization to Fourier series representations of $b_i(t)$

is then employed for further convenience.

Accordingly, the components of the perturbation field will take the form

$$b_{oi} = \sin\theta \sum_{n=n_o}^{N} a_{in} \cos\left[n\Omega_S t + n\theta + n\phi + \delta_{in}\right] \qquad (8)$$

$$i = r,\ \theta,\ \phi$$

Here $n\Omega_S = 2\pi f$ so that $n_o = 2\pi f_o/\Omega_S$, where f_o is the low-frequency limit of the frequency range of interest. The factor, $\sin\theta$, has been included in order to insure that ∇b_{oi} remains finite near the poles, i.e., near $\theta = 0$, although effects at low latitudes are the primary concern here. Then the three components of the perturbation field, $\vec{b}$, are

$$b_r = (r_o/r)^2 b_{or}\,(\theta,\ \phi,\ t-\Delta t)$$

$$b_\theta = (r_o/r)\ b_{o\theta}(\theta,\ \phi,\ t-\Delta t)$$

$$b_\phi = -(r_o/r)^2\ (\tan\alpha_p) b_{or}(\theta,\ \phi,\ t-\Delta t) + (r_o/r) b_{o\phi}(\theta,\ \phi,\ t-\Delta t)$$

where as before

$$\Delta t = (r-r_o)/V_p$$

The coefficients, a_{ij}, in the Fourier series representation of b_{oi} may be determined from the estimates of the power spectra of $B_i(t)$ that were described in Part 1. Let $dP_i(f)/df$ be spectral density of the power in the ith vector component of $\vec{B}(t)$. Then the coefficients may be evaluated from expressions of the form

$$[dP_r(f_n)/df]\Delta f = (r_o/r_1)^4 \, (\sin^2 \theta_1) \, (a_{rn}{}^2/2)$$

$$[dP_\theta(f_n)/df]\Delta f = (r_o/r_1)^2 (\sin^2 \theta_1)(a_{\theta n}{}^2/2) \qquad (10)$$

$$[dP_\phi(f_n)/df]\Delta f = (r_o/r_1)^4 \, (\tan^2 \alpha_p) \, (\sin^2 \theta_1)(a_{rn}{}^2/2)$$

$$+ \, (r_o/r_1)^2 \, (\sin^2 \theta_1) \, (a_{\phi n}{}^2/2)$$

where r_1 and θ_1 are coordinates of the position of the spacecraft at the time that $\vec{B}(t)$ was measured. During the flight, as shown in Figures 1 and 2 of Part 1, $0.70 \leq r \leq 1.0$ AU and $82° \leq \theta \leq 98°$. On Day 285, $r_1 = 1.4 \cdot 10^{13}$ cm and $\theta_1 = 82°$.

The index n, and the frequency f_n are related by the expression,

$$f_n = nf_o = f_o + (n-1)\Delta f$$

where Δf is the range of frequencies over which an individual estimate of the power density is obtained. Thus, the lower limit for Δf in Equations 10 is determined by the frequency resolution of the corresponding power spectrum. The frequency f_o is given by

$$f_o = f_N - N\Delta f$$

where f_N is the Nyquist frequency. In practice, we will use $N_{max.} = 1000$, corresponding to $f_o = f_n \cdot 10^{-3} = 1.35 \cdot 10^{-5}$ cps, or 1.16 cycles per day.

Equations 10, with $\theta = 90^\circ$, were employed to evaluate the coefficients a_{in}. The required values of $dP_i(f)/df$ were obtained from idealizations of the composite quiet-field spectra that are plotted in Figures 16 - 18 of Part 1. The idealized spectra, also shown in the figures, are given by

$$dP_i(f)/df = 10^5(f_o/f),\ 0.5f_o \leq f \leq 50f_o$$

$$dP_i(f)/df = 2 \cdot 10^3(50f_o/f)^2,\ 50f_o < f \leq 500f_o \qquad (11)$$

$$dP_i(f)/df = 0,\ f > 500\ f_o$$

for $i = r, \theta, \phi$. Here $f_o = f_N/1000$. In the Fourier-series approximation to the b_{oi}'s, given by Equations 8, one hundred coefficients were employed. The coefficients are given in Table 1.

The frequency dependence, f^{-2}, employed here for $50f_o < f \leq 500f_o$ is slightly stronger than that actually exhibited by the experimentally determined spectra. More recent evidence from OGO-1 [Holzer, McLeod, and Smith, 1966] suggests that the frequency dependence is slightly weaker than f^{-2} out to frequencies near the proton cyclotron frequency of 0.08 cps at which it steepens sharply and probably exhibits a cutoff. However, the variations at these higher frequencies are so small that the simplifying approximations used in Equations 11 are not expected to significantly affect the results here. Note also that we have employed the same spectra for B_r, B_θ, and B_ϕ although the variations in B_θ and B_ϕ were usually greater by factors of about 1.3 than those in B_r.

In a similar manner, a value for B_{so} may be obtained from the measurements of $B_r(t)$. Thus,

$$B_r(t) = (r_o/r)^2 B_{so} + b_{or}$$

and, since the time average of b_{or} is zero, the average value of $B_r(t)$ is just

$$\langle B_r(t) \rangle = (r_o/r)^2 B_{so}$$

The values of $\bar{B}_{r1}$ and $\bar{B}_{r2}$ listed in Table 1 of Part 1 indicate that

$$|\langle B_r(t)\rangle| \approx 3.0\gamma$$

during Solar Rotation Period 1768. From Figure 1 of Part 1, the average heliocentric range of the spacecraft was $140 \cdot 10^6$ km. Thus,

$$B_{so} \approx [(1.4 \cdot 10^{13})^2/r_o^{\,2}] \cdot 3 \cdot 10^{-5} \text{ gauss} \tag{12}$$

As mentioned previously, this model is greatly idealized. However, the overall statistical properties of the model field are consistent with the properties observed in the field between the orbits of the earth and Venus. Specifically, the frequency spectra of the vector components of the model field were chosen to be approximately the same as the spectra measured in the quiet interplanetary field, except in frequencies with periods greater than one day. Also, with the exception of the θ component, the magnitudes of the constant components of the vector field have been chosen to agree with the averages exhibited by the corresponding components of the measured field during periods in which the interplanetary field was directed back toward the sun (negative polarity, as defined in Part 1) along the spiral-field direction. The average field strength during periods of greater solar activity is probably somewhat greater than that observed during the flight. Thus, we will let $|B_r| = 5\gamma$ at r = 1.0 AU. For convenience, we will let $\vec{B}_{so}$ be positive.

The use of this model to describe the field in the region between the orbit of Venus and the sun is presently without empirical justification. However, the evidence for long-term stability of the polarity patterns of the photospheric magnetic fields [Babcock and Babcock, 1955] and evidence that the sun's supergranulation pattern has a mean lifetime of about 10 hours [Leighton, 1963] suggested the use of this model.

One feature of the model field at r_o is of interest. It may be recalled, from Part 1, that the measured values of the power in each of the vector components $B_i(t)$ were generally within a factor of two, or so, of each other during any given period. According to our model for the spatial dependence of the frozen-in fields, this approximate equality at $r \approx 1$ AU indicates the averages of $|b_{o\theta}|$ and $|b_{o\varphi}|$ are smaller by factors of roughly (r_o/r) than the average of $|b_{or}|$. Since $|b_{or}|$ is somewhat smaller than B_{so}, and since (r_o/r) is expected to be 0.1 or less, the model field at r_o, then, is almost entirely radial.

The Motion of Charged Particles in the Model Interplanetary Field

In this section, we will estimate the heliocentric range of the region of maximum scattering for protons of any particular energy moving through the interplanetary field described by our model. Specifically, the interplanetary field $\vec{B}(r, \theta, \phi, t) = \vec{B}_s + \vec{b}$, composed of the background spiral field, $\vec{B}_s$, and a perturbation field, $\vec{b}$, has components:

$$B_r(r, \theta, \phi, t) = B_{sr}(r) + b_r(r, \theta, \phi, t)$$

$$= (r_o/r)^2 \, [B_{so} + b_{or}(r, \theta, \phi, t)]$$

$$B_\theta(r, \theta, \phi, t) = b_\theta(r, \theta, \phi, t) \tag{13}$$

$$= (r_o/r) \, b_{o\theta} \, (r, \theta, \phi, t)$$

$$B_\phi(r, \theta, \phi, t) = -(\tan \alpha_p)[B_{sr}(r) + b_r(r, \theta, \phi, t)]$$

$$+ b_\phi(r, \theta, \phi, t)$$

$$= -(\tan \alpha_p) \, (r_o/r)^2 \, [B_{so} + b_{or}(r, \theta, \phi, t)]$$

$$+ (r_o/r) \, b_{o\phi}(r, \theta, \phi, t)$$

where $\tan \alpha_p = (\Omega_S/V_p) \, (r-r_o) \sin \theta$ and the components $b_{oi}(r, \theta, \phi, t)$, for $i = r, \theta, \phi$, are approximated by the Fourier series described in Table 1.

A charged particle with velocity v will move adiabatically in a magnetic field if the following conditions, given in terms of a coordinate system fixed relative to a line of force, are satisfied:

$$(T_g/B)\ (\partial B/\partial t) \ll 1$$

$$(R_g/B)\ |(\Delta B)_\perp| \ll 1$$

$$(T_g v_\parallel/B)\ |(\Delta B)_\parallel| \ll 1$$

[See, for example, Alfvén and Falthammar, 1963]. The subscripts '$\perp$' and '$\parallel$' are used to denote the directions transverse and parallel, respectively, to the line of force. The quantity T_g is the period of gyration for a particle of mass m and charge e in a field of strength B. Thus,

$$T_g = 2\pi\gamma mc/|e|\ B$$

Also, R_g is the radius of gyration, or

$$R_g = \gamma mvc/|e|\ B$$

and

$$\gamma = [1 - (v^2/c^2)]^{-1/2}$$

Parker [1964] has shown theoretically that the scattering of a charged particle by an irregularity in a magnetic field, if considered as a function of the energy or rigidity of the particle, exhibits a maximum value. Specifically, as the particle energy increases from adiabatic values, the scattering increases from zero to a maximum value and decreases, approaching zero again as the energy approaches relatively high values. The maximum scattering occurs for the particle energy at which the particle cyclotron frequency is just equal to $\partial B/\partial t$, measured in the frame of reference moving with the particle.

But resonance of this type is just the situation represented by the inequalities given above if the left-hand sides are set equal to unity. Thus, in the rest frame, the resonance occurs for

$$(T_g/B)\ (\partial B/\partial t) = 1$$

$$(R_g/B)\ |(\Delta B)_\perp| = 1 \tag{14}$$

$$|T_g v_\parallel/B|\ |(\Delta B)_\parallel| = 1$$

In the following then, using these equations, we wish to estimate the distance from the sun at which a particle of a particular energy will encounter such a resonance, i.e., maximum scattering, in the model interplanetary field.

We have

$$B = (B_r^{\,2} + B_\theta^{\,2} + B_\phi^{\,2})^{1/2}$$

$$= \{(B_{sr} + b_r)^2 + b_\theta^{\,2} + [b_\phi - (B_{sr} + b_r)\tan\alpha_p]^2\}^{1/2} \qquad (15)$$

so

$$(\partial B/\partial t) = (1/B)\,[B_r(\partial B_r/\partial t) + B_\theta(\partial B_\theta/\partial t) + B_\phi(\partial B_\phi/\partial t)]$$

$$= (1/B)\,\{(B_{sr} + b_r)\,(\partial b_r/\partial t) + b_\theta(\partial b_\theta/\partial t) \qquad (16)$$

$$+ [b_\phi - (B_{sr} + b_r)\tan\alpha_p]\,[(\partial b_\phi/\partial t) - (\partial b_r/\partial t)\tan\alpha_p]\}$$

In order to compute

$$\nabla B = \hat{e}_r(\partial B/\partial r) + \hat{e}_\theta(1/r)\,(\partial B/\partial\theta) + \hat{e}_\phi(1/r\sin\theta)\,(\partial B/\partial\phi) \qquad (17)$$

we require values of the rather cumbersome expressions

$$(\partial B/\partial r) = (1/B)[B_r(\partial B_r/\partial r) + B_\theta(\partial B_\theta/\partial r) + B_\phi(\partial B_\phi/\partial r)]$$

$$= (1/B)\ \{(B_{sr} + b_r)[\partial B_{sr}/\partial r) + (\partial b_r/\partial r)] + b_\theta(\partial b_\theta/\partial r) \qquad (18)$$

$$+ [b_\phi - (B_{sr} + b_r)\tan\alpha_p]\ [(\partial b_\phi/\partial r)(\partial B_{sr}/\partial r)(\tan\alpha_p)$$

$$- (\partial b_r/\partial r)(\tan\alpha_p) - (B_{sr} + b_r)\ (\partial \tan\alpha_p/\partial r)]\}$$

$$(1/r)\ (\partial B/\partial\theta) = (1/Br)[B_r(\partial B_r/\partial\theta) + B_\theta(\partial B_\theta/\partial\theta) + B_\phi(\partial B_\phi/\partial\theta)]$$

$$= (1/Br)\ \{(B_{sr} + b_r)\ (\partial b_r/\partial\theta) + b_\theta(\partial b_\theta/\partial\theta) \qquad (19)$$

$$[b_\phi - (B_{sr} + b_r)\tan\alpha_p][(\partial b_\phi/\partial\theta) - (\partial b_r/\partial\theta)\tan\alpha_p$$

$$- (B_{sr} + b_r)\ (\partial \tan\alpha_p/\partial\theta)]\}$$

and

$$(1/r\sin\theta)(\partial B/\partial\phi) = (1/Br\sin\theta)[B_r(\partial B_r/\partial\phi) + B_\theta(\partial B_\theta/\partial\phi)$$

$$+ B_\theta(\partial B_\theta/\partial\phi)] \qquad (20)$$

$$= (1/Br\sin\theta)\ \{(B_{sr} + b_r)(\partial b_r/\partial\phi) + b_\theta(\partial b_\theta/\partial\phi)$$

$$+ [b_\phi - (B_{sr} + b_r)\tan\alpha_p]\ [(\partial b_\phi/\partial\phi)$$

$$- (\partial b_r/\partial\phi)\tan\alpha_p]\}$$

From Equations 13,

$$(\partial B_r/\partial r) = -2(1/r)\ (r_o/r)^2(B_{so} + b_{or}) + (r_o/r)^2(\partial b_{or}/\partial r)$$

$$(\partial B_r/\partial \theta) = (1/r)\ (r_o/r)^2\ (\partial b_{or}/\partial \theta)$$

$$(\partial B_r/\partial \phi) = (r_o/r)^2\ (\partial b_{or}/\partial \phi)$$

$$(\partial B_\theta/\partial r) = -(1/r)\ (r_o/r)b_{o\theta} + (r_o/r)\ (\partial b_{o\theta}/\partial r)$$

$$(\partial B_\theta/\partial \theta) = (r_o/r)\ (\partial b_{o\theta}/\partial \theta)$$

$$(\partial B_\theta/\partial \phi) = (r_o/r)\ (\partial b_{o\theta}/\partial \phi)$$

$$\begin{aligned}(\partial B_\phi/\partial r) = {} & -(1/r)\ (r_o/r)b_{o\phi} + (r_o/r)\ (\partial b_{o\phi}/\partial r) \\ & + (2/r)(r_o/r)^2 B_{so} \tan \alpha_p + (2/r)(r_o/r)^2 b_{or} \tan \alpha_p \\ & + (r_o/r)^2(B_{so} + b_{or})\ (\partial \tan \alpha_p/\partial r) \\ & - (r_o/r)^2\ (\partial b_{or}/\partial r) \tan \alpha_p\end{aligned}$$

$$\begin{aligned}(\partial B_\phi/\partial \theta) = {} & (r_o/r)(\partial b_{o\phi}/\partial \theta) - (r_o/r)^2(B_{or} + b_{or})(\partial \tan \alpha_p/\partial \theta) \\ & - (r_o/r)^2\ (\partial b_{or}/\partial \theta) \tan \alpha_p\end{aligned}$$

$$(\partial B_\phi/\partial \phi) = (r_o/r)\ (\partial b_{o\phi}/\partial \phi) - (r_o/r)^2\ (\partial b_{or}/\partial \phi) \tan \alpha_p$$

The b_{oi}'s are given in Table 1 and B_{so} is a constant, also listed in the table.

As in Part 1, we again introduce the coordinate system,

$w\theta v$, with unit vectors $\hat{e}_w$, parallel to the spiral-field line of force, $\hat{e}_\theta$, defined as in the $r\theta\phi$ system, and $\hat{e}_v$, completing the right-handed orthogonal system. Thus,

$$\hat{e}_w = \hat{e}_r \cos \alpha_p - \hat{e}_\phi \sin \alpha_p$$

$$\hat{e}_\theta = \hat{e}_\theta \tag{21}$$

$$\hat{e}_\phi = \hat{e}_r \sin \alpha_p + \hat{e}_\phi \cos \alpha_p$$

In terms of the unit vectors in this system the spiral field is simply $\vec{B}_s = \hat{e}_w B_s$ where the field strength is

$$B_s(r, \theta) = B_{so}(r_o/r)^2 [1 + \tan^2 \alpha_p]^{1/2} \tag{22}$$

We may obtain $(\nabla B)_\parallel$, using Equations 21 from

$$(\nabla B)_\parallel = \nabla B \cdot \hat{e}_w$$

and $(\nabla B)_\perp$ from

$$|(\nabla B)_\perp| = [(\nabla B)^2 - (\nabla B)_\parallel{}^2]^{1/2}$$

For a particle of mass m, charge e, and pitch angle χ, the upper limits on energy for adiabatic motion may be obtained from Equations 14. Substituting time averages for $\partial B/\partial t$ and the components of ∇B and rearranging, we obtain

$$\gamma = (e/mc)\ (1/2\pi)[\langle B^4/(\partial B/\partial t)^2\rangle]^{1/2} \tag{23}$$

$$\gamma v \sin\chi = (e/mc)\ [\langle B^4/(\nabla B)_\perp{}^2\rangle]^{1/2} \tag{24}$$

$$\gamma v \cos\chi = (e/mc)\ (1/2\pi)\ [\langle B^4/(\nabla B)_\parallel{}^2\rangle]^{1/2} \tag{25}$$

The time averages were evaluated under the assumption that the variations in the vector components of the field were independent of one another. As discussed in Parts 1 and 2 [Coleman, 1966], this assumption is not strictly accurate. However, the coherences between the vector components were low enough to be neglected for our present purposes. In computing the various time averages, expressions of the form $\langle(1/B)^2\ (\partial B/\partial x)^2\rangle$ were approximated by $(1/B_s)^2\ \langle(\partial B/\partial x)^2\rangle$. Here $x = r,\ \theta,\ \phi,\ t$.

Thus, the right-hand sides of Equations 23 - 25 were evaluated for protons in the field $\vec{B} = \vec{B}_s + \vec{b}$. Then, for various values of the pitch angle χ, the values of γ were obtained and used to determine the values of E from

$$E = mc^2\ (\gamma - 1)$$

The resulting values of E are plotted as functions of r for $\chi = 1$, 45, and 89°, in Figure 1 for $\delta = 0$, i.e., in the solar equatorial plane. The values of E determined from Equation 23 are denoted by E_{mt}. The values determined from Equations 24 and 25 are denoted, respectively, by $E_{m\perp}$ and $E_{m\parallel}$. Thus, for any heliocentric range, $r = r_1$, a proton of pitch angle $\chi = 45^\circ$, for example, would be efficiently scattered if it had an energy approximately equal to one of three values, $E_{mt}(r = r_1)$, $E_{m\parallel}(\chi = 45^\circ,\ r = r_1)$, or $E_{m\perp}(\chi = 45^\circ,\ r = r_1)$ from the appropriate curves in Figure 1. From the curve for E_{mt} versus r in Figure 1, it is apparent that we may neglect the effects of the temporal variations in the model field except for protons of rather high energies.

In Figure 2, the shaded areas show the ranges of heliocentric distance over which maximum scattering may occur for a proton of a given energy. (Here E_{mt} is neglected.) The particular value or values of r within the shaded area, at which scattering would be most efficient, depend only upon the pitch angle. In Figure 2, Region A is the region enclosed by the curves of $E_{m\parallel}$ for $\chi = 1$ and 89°. Region B is the region enclosed by the curves of $E_{m\perp}$ for these two values of χ.

A comparison of the inequalities that define adiabatic motion with Equations 14 or the approximations to Equations 14 given by Equations 23, 24, and 25, showsthat the values of E_{mt}, $E_{m\perp}$, and $E_{m\parallel}$ are just the extreme upper limits for the ranges of energies over which adiabatic motion is possible. It is desirable to estimate the fraction of E_{mi}, $i = t, \parallel, \perp$, at which non-adiabatic behavior would become significant. In this connection, Northrop [1963] has discussed the motion of charged particles in static, magnetic mirror machines. Some instability evidently occurs when the ratio of the gyro radius of the particle to the distance between the mirrors exceeds 0.03. For purposes of this discussion, then, it will be assumed that the particles with pitch angle χ perform ideal adiabatic motion at the point (r, θ, ϕ) if their energies are less than $(0.03)^2 E_{mi} \approx 10^{-3} E_{mi}$.

Thus, for example, the motion of a proton with $\chi = 45°$ and energy 10^2 Mev, would begin to deviate from adiabatic motion at a distance from the sun defined by the intersection of the horizontal line $E = 10^5$ Mev and the curve for $E_{m\parallel}$ with $\chi = 45°$, or at $r \approx 0.15$ AU. However, it would not reach a region of efficient scattering until it travels beyond 6 AU. Figure 1 shows that the distance beyond 6 AU would be very great for protons of small pitch angles.

From Figure 2, assuming that the protons behave adiabatically for $E \leq 10^{-3} E_m$, it would appear that particles with $E \leq 1$ Mev, which reach $r > 2$ AU with pitch angles smaller than a few degrees, will travel freely outward through interplanetary space at least to 100 AU. This means that most protons with energies in this range will move adiabatically throughout interplanetary space, in the model field, since even those which have pitch angles nearly 90° while near the sun will reach 2 AU with pitch angles of less than 1°. Under the same assumption, Figure 2 shows that solar protons with E ≈ 100 Mev would begin to scatter at a heliocentric range between 0.13 and 0.26 AU, regardless of pitch angle. Protons with higher energies would begin to scatter closer to the sun while those with energies between 100 and 1 Mev will start to scatter at ranges between 0.13 and roughly 2 AU. Note that non-relativistic solar electrons would move adiabatically throughout interplanetary space, since the curves shown for protons apply to electrons with the same momenta or with energies that are greater than those given by a factor of $m_p/m_e = 1836$.

Discussion

As a first step in relating the results of the preceding section to the observed behavior of solar cosmic rays, we will briefly describe some pertinent aspects of this behavior. The probability that particles ejected during a particular solar flare will reach the vicinity of the earth is a function of the position of the parent flare. If flare particles reach the earth, the time of arrival and the time to maximum intensity, measured relative to the onset of the flare, is also related to the position of the parent flare. In general, the west-limb flares are more effective at producing detectable fluxes with shorter delays from the onset of the flare to the arrival and subsequent intensity peak of the flare particles [McCracken, 1959; Reid and Leinbach, 1959; Obayashi and Hakura, 1960; McCracken and Palmeira, 1960]. The overall spiral configuration of the interplanetary field, as described by Parker [1958], is evidently responsible for this dependence upon the position of the parent flare.

In several cases, the initial directional intensity of the solar-flare particles reaching the earth has been observed to be strongly anisotropic. Two such events, May 4 and November 15, 1960, have been described in detail by McCracken, [1962]. In both these events, relativistic particles were produced by the flares so that the fluxes at the earth could be detected by neutron monitors on the surface. An initial anisotropy was also detected in the directional intensities of particles of lower energies following the flare of September 28, 1961, [Bryant, Cline, Desai, and McDonald, 1962]. These measurements were obtained with earth-satellite instruments. This anisotropy is evidently a relatively unusual condition. It occurs only when the parent flare is located near the source of lines of force in the interplanetary field that also pass near the earth. In each of the three cases, the directional intensity was subsequently observed to approach isotropy.

Following the arrival of the first particles at the earth, regardless of the initial isotropy or lack thereof, the intensity usually reaches a maximum within a few hours and then decreases much more slowly, suggesting decay times in the range between hours and days. Details of the time dependence of the intensity of solar-flare cosmic rays have been described for a number of events. Examples may be found in Meyer, Parker, and Simpson, [1956], Winckler and Bhasvar, [1963], Arnoldy, Hoffman, and Winckler, [1960], Anderson and Enemark, [1960], Lin and Van Allen, [1963], Bryant, Cline, Desai, and McDonald, [1965], and Krimigis, [1965].

Many of the recent interpretations of solar cosmic-ray effects have involved particle diffusion or scattering by magnetic-field irregularities. These phenomena are employed in order to account for the long decay times mentioned previously. As additional background for the discussion of our results, a few of these interpretative models will next be briefly described. Parker [1963] has proposed a model for the quiet interplanetary field in which the field between the sun and perhaps 1 - 2 AU is, for the most part, smooth and radial, or spiraled, and in which the field beyond this boundary is mainly azimuthal and disordered throughout a thick, spherical shell extending to interstellar space. The particle diffusion occurs in this shell. Diffusion within this shell permits particles injected into a tube of flux of the spiral field to appear on other distant lines of force without crossing the well organized spiral field. The particles simply travel outward to the disordered shell, diffuse around the shell, and, in some cases re-enter the inner solar system on different lines of force in the spiral field. Leakage outward across the outer boundary of the shell then accounts for the gradual decay of the solar cosmic-ray intensity.

Reid [1964] has described a model in which distribution of the particles is accomplished by diffusion through a region in the solar atmosphere so that the injection of the particles in the spiral field actually occurs over a much wider area than that occupied by the active region. In this model, the particles apparently diffuse through the chromospheric magnetic fields.

Krimigis [1965] has compared a different version of Parker's diffusion model with various observations. In this version, the diffusive medium extends outward from the sun to several AU. As in the other two models, the diffusion is produced by irregularities in the ambient magnetic field that form effective scattering centers for charged particles.

Evidence for scattering by field irregularities in the inner solar system region has been obtained by McCracken [1962] from the previously mentioned analysis of promptly arriving solar-flare particles. It was found that the orientation of the axis of symmetry of the directional intensity was about the orientation expected for a typical spiral field. However, the range of the directions of arrival was found to cover a cone of half-angle 80°. It was concluded that this range indicated an equal range in the pitch angles of the arriving particles coming directly from the sun could only result from scattering by field irregularities along the particle trajectories at considerable distances from the sun. McCracken also cited evidence, from the events of February 23, 1956, [Lust and Simpson, 1957] and July 17, 1959 [Brown and D'Arcy, 1959], for a dependence of the 'apparent' pitch angle upon particle rigidity. Specifically, it was shown that the apparent pitch angle increased with increasing rigidity until the rigidity was about 1.1 bv and decreased with increasing rigidity about this value.

We would emphasize that the dependence of the apparent scattering upon rigidity is the significant feature of this evidence for the existence of scattering, since the variability of the orientation of the interplanetary field, during a period of an hour or so, is typically sufficient to cause particles to arrive from directions differing by 60° or more from the nominal spiral-field direction. The distributions of the 3-hr, rms deviations, the magnitudes of the vector components in the w, θ, v system showed typical values during the flight as follows:

$\sigma(B_w) \approx 2.0$

$\sigma(B_\theta) \approx 1.8$

$\sigma(B_v) \approx 1.5$

Since B_s is about 4.0γ, a reasonable maximum value for the angle between the $\vec{B}_w$ and $\vec{B}$ is

$$\tan^{-1}[(4.0 - 2.0\sqrt{2})/1.8\sqrt{2}] \approx 70°$$

As may be seen from the results presented in Part 1, this angle can easily be greater. The angle from the spiral-field direction to the actual field was denoted by β_B in Part 1. The distribution of the values of this angle during SRP 1768 is show in Figure 11 of Part 1. Note that the values of β_B near 90° were recorded frequently.

The variability of this angle indicates that particles moving adiabatically along the lines of force, with pitch angles near 0°, may often arrive from directions differing by 80°

from the nominal spiral-field direction during any period of a few hours. For this reason the dependence of the apparent pitch angle, or scattering angle, upon rigidity is the strongest evidence for the occurrence of scattering by the field between the sun and the earth.

In any case, McCracken found that particles of energies near 450 Mev exhibited the greatest apparent scattering. As shown in Figure 1, our model for a typical field configuration indicates that protons with energies in the range 1 - 2 Bev and pitch angles in the range 0 - 45° will encounter the most efficient scattering at r = 1 AU. Protons with energies of 5 to 9 Bev would also be scattered efficiently if any were present with pitch angles in the range 45 to 90°.

Although the values of 450 Mev and 1 Bev are satisfactorily close to equality, it must be kept in mind that the calculations here do not allow us to determine the integrated effects of scattering in the region between the sun and 1 AU, and it is the integrated effects that determine the directional spectral intensity at 1 AU. Thus, the rough agreement between the 'energy of maximum scattering' observed at 1 AU and energies for which the scattering by the field is most efficient at 1 AU may not be particularly significant, since the former is determined by the integrated effect of scattering between the sun and 1 AU, while the latter is determined by the scattering efficiency at 1 AU.

Let us consider next the models involving diffusion of the solar-flare particles in the light of the results of the preceding section. Of the three, one requires diffusion through the solar atmosphere. Since our results have no direct bearing upon this model, we will consider further only the other two. One of these models requires diffusion in the inner solar system and the other requires a small amount of scattering in this region and diffusion in a thick, spherical shell well beyond 1.0 AU. Thus, in the latter model the field inside 1.0 AU is essentially a smooth, spiral field. A comparison between the spiral-field model and the observations described herein has been provided in Part 1. The observations have established the existence of substantial perturbations about the spiral-field configuration inside 1.0 AU. The question at hand is whether these perturbations are sufficient to produce diffusion of solar cosmic rays through the inner solar system.

As mentioned previously, the model that requires diffusion in this region has been examined in some detail by Krimigis [1965], who compared the behavior of solar cosmic rays indicated by the model with the behavior observed during the event of September 28, 1961. The comparison provides indirect evidence concerning various properties of the field irregularities between the sun and the earth. In deriving this diffusion model used by Krimigis, Parker [1961] assumed that the solar-flare particles perform an isotropic random walk through a field of static irregularities the density of which depends only upon r, the distance from the sun. It was further assumed that the resulting particle diffusion was described by a diffusion coefficient given by Mr^{β} where M and β are functions of the particle energy E. Given solutions of the resulting diffusion equation and the observed time dependence of the spectral intensity of the solar cosmic rays near the earth, Krimigis obtained values of the two parameters in the diffusion coefficient for various particle energies.

For the event of September 28, 1961, it was concluded that β was independent of E for $E > 55$ Mev and that, at $r = 1$ AU, the diffusion coefficient was nearly constant for $40 < E < 55$ Mev, but increased as $E^{0.33}$ for $55 < E < 450$ Mev. The value $E = 450$ Mev was evidently about the highest recorded during the event.

Now the diffusion coefficient for particles executing isotropic random walk in a static scattering medium can be written $\lambda v/3$ where λ is the mean free path of a particle and v is its velocity [Parker, 1963]. The energy dependence of the diffusion coefficient and the velocity for $E > 55$ Mev indicate that λ decreases rapidly with increasing E for $E > 55$ Mev, flattens out and approaches a constant value of 0.08 AU at $E = 450$ Mev.

A decrease in the mean free path indicates an increase in the scattering. Thus, the minimum value of λ will be the mean free path of the particles that suffer the most scattering. This result leads to the conclusion that the value of $E = 450$ Mev, at which λ appeared to reach a constant value, was probably not much smaller than the energy at which maximum scattering would have occurred. That is, if the particles with E considerably greater than 450 Mev had been observed, the value of λ for these particles would have been greater.

In other words, for the event of September 28, 1961, the diffusion model suggests that, at 1 AU, the smaller of the resonant energies $E_{m\parallel}$ and $E_{m\perp}$ was somewhat greater than 450 Mev. Thus, values of $E = 1 - 2$ Bev obtained for maximum scattering at $r = 1.0$ AU, are in satisfactory agreement. Recall that this same approximate value of 450 Mev was assigned to the particles that exhibited the greatest apparent scattering during the events studied by McCracken.

As discussed previously, it is apparent from Figure 2, that solar protons at 1 AU with $E \approx 1$ Mev would not show any scattering effects. However, the scattering would increase with energy, probably slowly at first, to $E_{m\parallel}$ ($\chi = 1°$, $r = 1$ AU) ≈ 1 Bev. This energy dependence of the scattering at 1 AU is also in rough agreement with that discussed above, based upon estimates of the diffusion coefficient at 1 AU.

The results of this comparison indicate that variations in the quiet interplanetary field, such as those observed particles exhibit resonances with the field irregularities.

The integrated effects of the scattering will not be accurately determined here. However, from Figure 2, it is apparent that a particle of energy E may always encounter a region of maximum scattering between the sun and interstellar space, since any line of constant E crosses either Region A or Region B, or both. These areas define regions of maximum diffusive resistivity, since, within the range of r so defined, protons are most likely to encounter the most effective scattering and diffusion regardless of their pitch angles. Thus, the maximum dynamical friction or resistance to the progress of the particle in the radial direction is likely to be encountered in this region.

A number of the effects observed in the directional spectral intensity of solar-flare protons may be interpreted in terms of the properties of Regions A and B without recourse to a formal derivation of a diffusion coefficient. Consider first, particles with energies greater than 10 Bev. These particles will encounter Region A somewhere inside 0.7 AU. As a result, their arrival at 1 AU will be delayed somewhat, and they will show the integrated effects of their traversal of the region. A determination of the length of the delay, the magnitude of the scattering, etc., must await the derivation of an expression for the diffusion coefficient. The 10-Bev particles that reach

1 AU with small pitch angles are relatively free to travel outward through Region B to distances as great as 20 AU, where they again encounter some efficient scattering. Thus, the time dependence of the directional spectral intensity of these particles will be determined partly by the source of the particles and by the diffusion at $r < 1$ AU and partly by the diffusion at $r > 1$ AU.

Consider next particles with energies less than 100 Mev. These particles will not encounter Region A at all, and they will not encounter Region B until they are well beyond 1 AU. However, they may begin to scatter inside 1 AU, according to the rather restrictive assumption that scattering effects will set in at $E \approx 10^{-3} E_{mi}$. Thus, the properties of the solar protons at 1 AU with energies less than 100 Mev will be determined by the source and the diffusion at $r > 1$ AU primarily, with little dependence upon diffusion at $r < 1$ AU.

As mentioned previously, in order to account for the delayed arrivals of isotropic fluxes of flare particles with energies in the 1 - 100 Mev range and at the same time account for the long decay time of the intensity of these particles, Parker suggested that a thick, diffusive shell might exist somewhere beyond 1 AU. But the properties required of the shell are just those that might be expected of Region B. For example, the fields in Region B could scatter the lower energy particles back toward the sun. Thus, the fields described by the model may account for the diffusive distribution of the flare particles and the long decay times, thereby eliminating requirements for special mechanisms such as instabilities or shocks which were assumed to be capable of developing such a diffusive shell.

A precise comparison of the observed cosmic-ray effects and the effects expected to be produced by the model field must await the derivation of an explicit diffusion coefficient for the model. However, on the basis of this qualitative discussion, it would appear that many of the variations in the directional spectral intensities of solar-flare protons may be explained in terms of this relatively simple model for the quiet interplanetary field.

Acknowledgments

This work was supported by the National Aeronautics and Space Administration under Research Grant NsG 249.

References

Alfvén, H., and C.G. Fälthammar, Cosmical Electrodynamics, Fundamental Principles, Clarendon Press, Oxford, 1963.

Anderson, K.A., and D.C. Enemark, Observations of solar cosmic rays near the north magnetic pole, J. Geophys. Res., 65, 2657-2671, 1960.

Arnoldy, R.L., R.A. Hoffman, and J.R. Winckler, Solar cosmic rays and soft radiation observed at 5,000,000 kilometers from earth, J. Geophys. Res., 65, 3004-3007, 1960.

Babcock, H.W., and H.D. Babcock, The sun's magnetic field, 1952-1954, Astrophys. J., 121, 349-366, 1955.

Brown, R.R., and R.G. D'Arcy, Observations of solar flare radiation at high latitude during the period July 10-17, 1959, Phys. Rev. Letters, 3, 390-392, 1959.

Bryant, D.A., T.L. Cline, U.D. Desai, and F.B. McDonald, Explorer 12 observations of solar cosmic rays and energetic storm particles after the solar flare of September 28, 1961, J. Geophys. Res., 67, 4983-5000, 1962.

Bryant, D.A., T.L. Cline, U.D. Desai, and F.B. McDonald, Studies of solar protons with Explorers 12 and 14, Astrophys. J., 141, 478-499, 1965.

Chandrasekhar, S., Stochastic problems in physics and astronomy, Rev. Mod. Phys., 15, 1-87, 1943.

Coleman, P.J., Jr., Variations in the interplanetary magnetic field: Mariner 2, Part 1. Observed properties, Publication No. 501, Institute of Geophysics and Planetary Physics, University of California, Los Angeles, 1966.

Coleman, P.J., Jr., Variations in the interplanetary magnetic field: Mariner 2, Part 2. Interpretation in terms of hydromagnetic waves, Publication No. 504, Institute of Geophysics and Planetary Physics, University of California, Los Angeles, 1966.

Holzer, R.E., M.G. McLeod, and E.J. Smith, Preliminary results from the Ogo 1 search coil magnetometer: Boundary positions and magnetic noise spectra, J. Geophys. Res., 71, (5), 1481-1486, 1966.

Krimigis, S.M., Interplanetary diffusion model for the time behavior of intensity in cosmic ray event, J. Geophys. Res., 70, 2943-2960, 1965.

Leighton, Robert B., The solar granulation, Annual Review of Astronomy and Astrophysics, 1, 19-40, 1963.

Lin, W.C., and J.A. VanAllen, Observation of solar cosmic rays from October 13, 1959, to February 17, 1961, with Explorer 7, Proc. Intern. School Phys. Enrico Fermi Course XXIV: Space Exploration and the Solar System, 194, Academic Press, New York, 1963.

Lust, R., and J.A. Simpson, Initial stages in the propagation of cosmic rays produced by solar flares, Phys. Rev., 108, 1563-1576, 1957.

McCracken, K.G., A correlation between the emission of white light and cosmic radiation by a solar flare, Nuovo Cimento, 13, 1081-1085, 1959.

McCracken, K.G., Cosmic ray flare effect: Parts 2 and 3, J. Geophys. Res., 67, 435-458, 1962.

McCracken, K.G., and R.A.R. Palmeira, Comparison of solar cosmic-ray injections including July 17, 1959, and May 4, 1960, J. Geophys. Res., 65, 2673-2683, 1960.

Meyer, P.E., E.N. Parker, and J.A. Simpson, Solar cosmic rays of February 1956 and their propagation through interplanetary space, Phys. Rev., 104, 768-783, 1956.

Northrop, T.G., The Adiabatic Motion of Charged Particles, Number 21, Interscience Publishers, New York, 1963.

Obayashi, T., and Y. Hakura, Propagation of solar cosmic rays through the interplanetary magnetic field, J. Geophys. Res., 65, (10), 3143-3148, 1960.

Parker, E.N., Dynamics of the interplanetary gas and magnetic fields, Astrophys. J., No. 128, 664-676, 1958.

Parker, E.N., Sudden expansion of the corona following a large solar flare and the attendant magnetic field and cosmic ray effects, Astrophys. J., 133, 1014-1033, 1961.

Parker, E.N., Interplanetary Dynamical Processes, Interscience Publishers, New York, 1963.

Parker, E.N., The scattering of charged particles by magnetic irregularities, J. Geophys. Res., 69, 1755-1758, 1964.

Reid, G.C., A diffusive model for the initial phase of a solar proton event, J. Geophys. Res., 69, 2659-2667, 1964.

Reid, G.C., and H. Leinbach, Low-energy cosmic-ray events associated with solar flares, J. Geophys. Res., 64, (11), 1801-1805, 1959.

Winckler, J.R., and P.D. Bhasvar, The time variations of solar cosmic rays during the September 3, 1960, event, J. Geophys. Res., 68, 2099-2115, 1963.

Table 1

The Vector Components of the

Model Interplanetary Field

$$B_r = (r_o/r)^2 \; (B_{so} + b_{or})$$

$$B_\theta = (r_o/r) \; b_{o\theta}$$

$$B_\phi = -(r_o/r)^2 \; (B_{so} + b_{or}) \tan \alpha_p + (r_o/r) b_{o\phi}$$

where

$$\tan \alpha_p = (r - r_o) \; (\Omega_S / V_p) \sin \theta$$

and

$$b_{oi} = \sin \theta \sum_{n=1}^{100} a_{in} \cos \{2\pi n f_o \, [t - (1/V_p) \, (r - r_o)$$

$$+ (\theta/\Omega_S) + (\phi/\Omega_S)] + \delta_{ni}\}$$

Here

$i = r, \theta, \phi$

$f_o = f_N/1000 = 1.35 \cdot 10^{-5}$ cps

$\Omega_S = 2.9 \cdot 10^{-6}$ rad/sec

$B_{so} = (r_1/r_o)^2 \; (5 \cdot 10^{-5})$ gauss

δ_{ni} is an arbitrary phase angle

$r_1 = 1$ AU $= 149 \cdot 10^{11}$ cm

and

Table 1
(continued)

$$a_{rn} = (r_1/r_o)^2 c_n$$

$$a_{\theta n} = (r_1/r_o)c_n$$

$$a_{\varphi n} = \{[1-(r_o/r_1)^2 (r_1-r_o) (\Omega_S/V_p)]^2 + (r_o/r_1)^2\}^{-1/2} c_n$$

where

$$r_1 = 1.4 \cdot 10^{13} \text{ cm}$$

and the c_n's are as follows: For n = 1,

$$c_1 = 2.66 \cdot 10^{-5} \text{ gauss}$$

For $2 \leq n \leq 10$,

$$c_n = 1.64 \cdot 10^{-5} \{\ln[(5n + 2.5)/(5n - 2.5)]\}^{1/2} \text{ gauss}$$

For $11 \leq n \leq 100$,

$$c_n = 4.24 \cdot 10^{-7} \{[1/(5n - 2.5)] - [1/(5n + 2.5)]\}^{1/2} \text{ gauss}$$

Figure Captions

Figure 1. Proton energies at which maximum scattering would occur in the model field. The values shown are those for the solar equatorial plane. Note that the values of E for E_{mt} are given on the right-hand side while those for $E_{m\perp}$ and $E_{m\parallel}$ are given on the left-hand side.

Figure 2. Regions of most efficient scattering for protons. For a particular energy, the values of r within the regions at which the most efficient scattering would occur depend upon the pitch angle. The values for a pitch angle of 45° are shown.

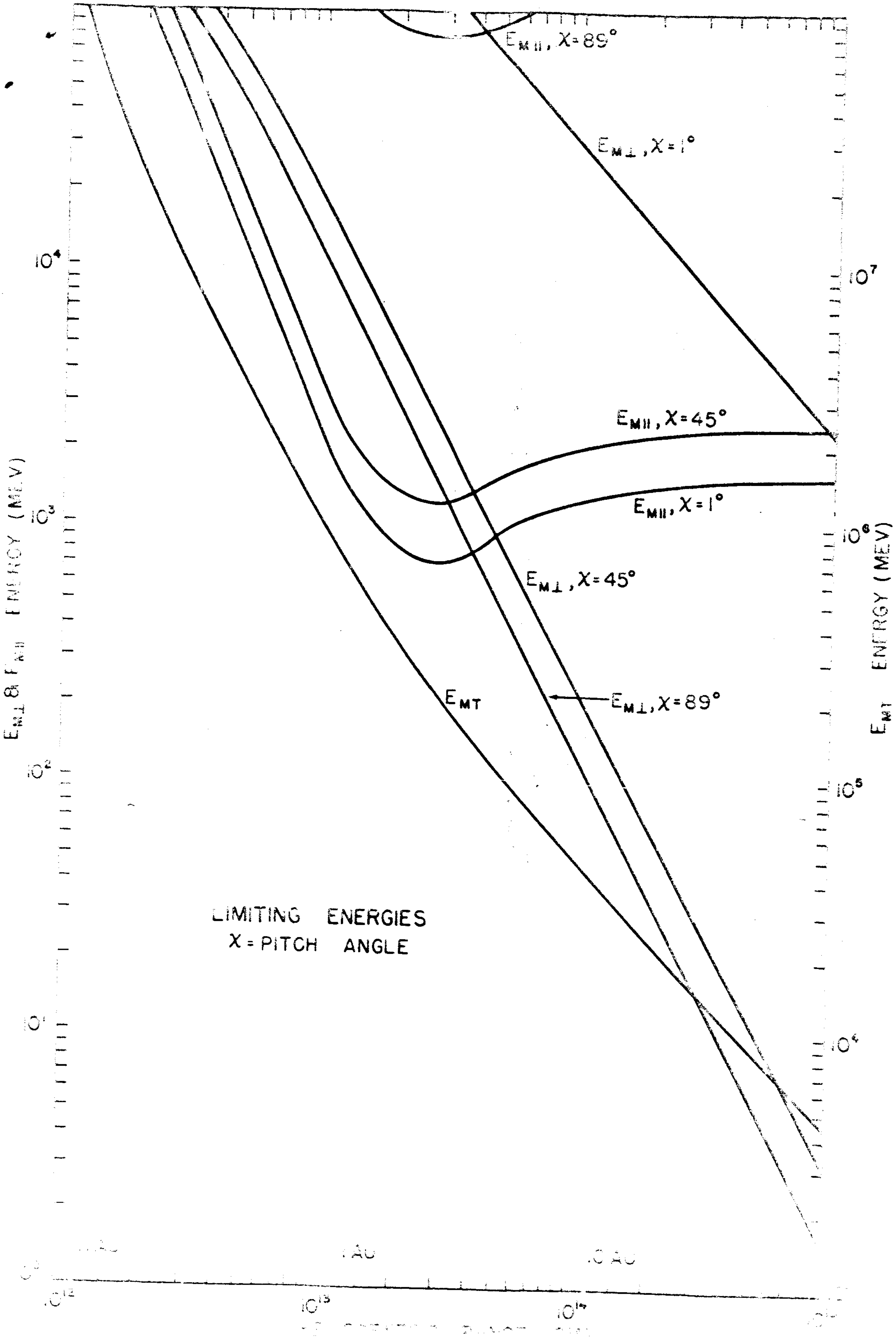

$E_{M\parallel}$, χ=89°
$E_{M\perp}$, χ=1°
$E_{M\parallel}$, χ=45°
$E_{M\parallel}$, χ=1°
$E_{M\perp}$, χ=45°
E_{MT}
$E_{M\perp}$, χ=89°
LIMITING ENERGIES
χ = PITCH ANGLE
10^4
10^3
10^2
10^1
10^7
10^6
10^5
10^4
E_{MT} ENERGY (MEV)
10^{13}
10^{14}

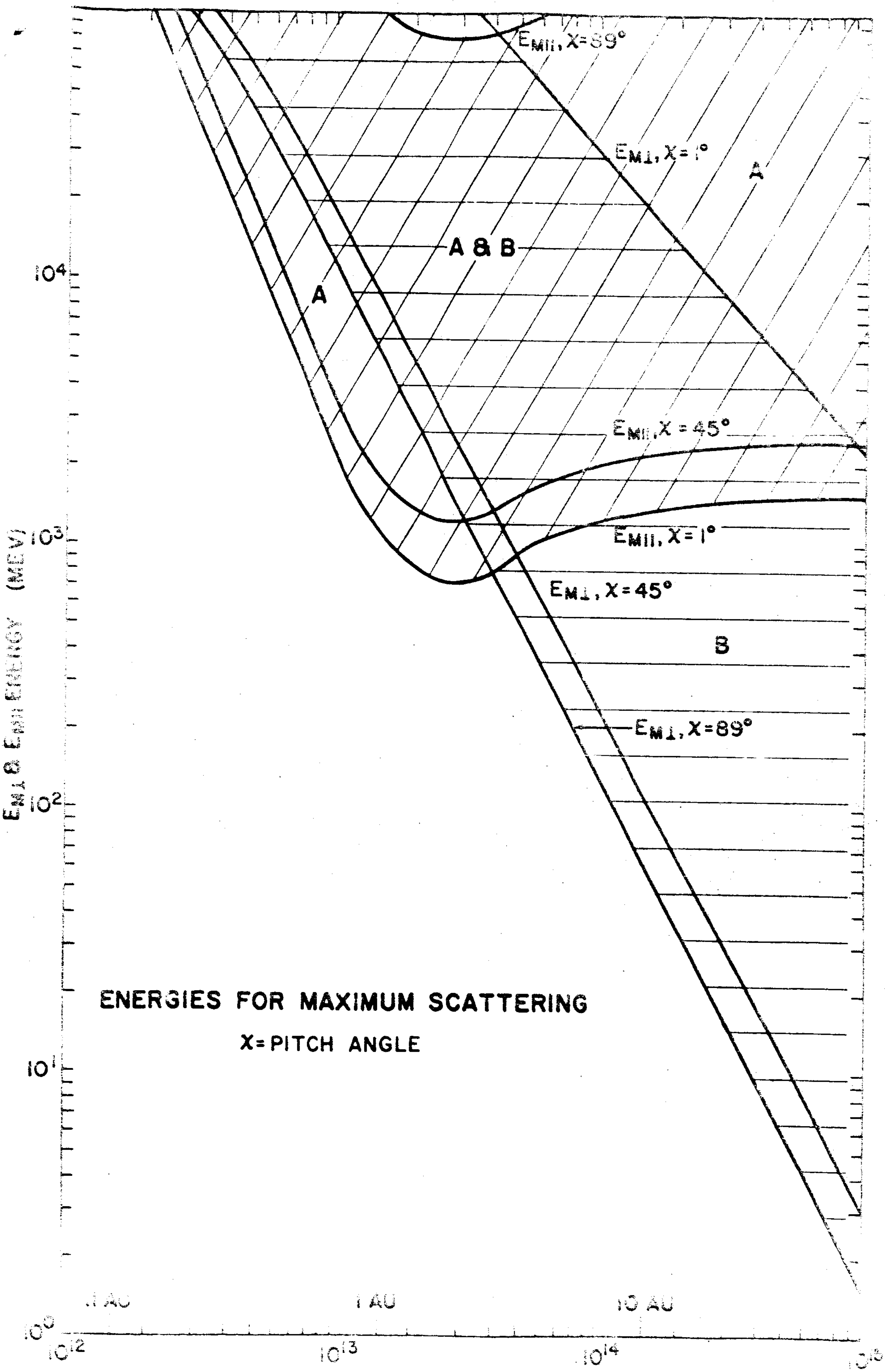

ENERGIES FOR MAXIMUM SCATTERING

X= PITCH ANGLE